Biochimica et Biophysica Acta 1827 (2013) 1174–1182

Contents lists available at ScienceDirect

Biochimica et Biophysica Acta

journal homepage: www.elsevier.com/locate/bbabio

The Tll0287 protein is a hemoprotein associated with the PsbA2-Photosystem II complex in *Thermosynechococcus elongatus*

Alain Boussac [a,*], Kazumi Koyama [b], Miwa Sugiura [b,c,**]

[a] *iBiTec-S, CNRS UMR 8221, CEA Saclay, 91191 Gif-sur-Yvette, France*
[b] *Proteo-Science Research Center, Ehime University, Bunkyo-cho, Matsuyama, Ehime 790-8577, Japan*
[c] *PRESTO, Japan Science Technology Agency (JST), 4-1-8, Honcho, Kawaguchi, Saitama 332-0012, Japan*

ARTICLE INFO

Article history:
Received 8 November 2012
Received in revised form 27 May 2013
Accepted 5 June 2013
Available online 14 June 2013

Keywords:
Photosystem II
PsbA
D1
Tll0287
Thermosynechococcus elongatus
Cyanobacterium

ABSTRACT

Cyanobacteria have multiple *psbA* genes encoding PsbA, the D1 reaction center protein of the Photosystem II (PSII) complex. The thermophilic cyanobacterium *Thermosynechococcus elongatus* has three *psbA* genes differently expressed depending on the environmental conditions. Among the 344 residues of PsbA, there are 21 substitutions between PsbA1 and PsbA3, 31 between PsbA1 and PsbA2 and 27 between PsbA2 and PsbA3. In this study, we found a new hemoprotein that is expressed when the *T. elongatus* genome has only the $psbA_2$ gene for D1. This hemoprotein was found in both the non-membrane proteins and associated to the purified PsbA2-PSII core complex. This protein could be removed by the washing of PSII with Tris-washing or $CaCl_2$-washing. From MALDI-TOF/TOF spectrometry, N-terminal sequencing and MALDI-MS/MS analysis upon tryptic digestion, the new hemoprotein was identified to be the *tll0287* gene product with a molecular mass close to 19 kDa. Until now, *tll0287* was registered as a gene encoding a hypothetical protein with an unknown function. From the amino acid sequence and the EPR spectrum the 5th and 6th axial ligands of the heme iron are the His145 and likely either the Tyr93, Tyr159 or Tyr165, respectively. From EPR, the heme containing Tll0287 protein associated to PsbA2-PSII corresponds to approximately 25% of the $Cytc_{550}$ content whereas, from SDS page analysis, the total amount of Tll0287 with and without the heme seems almost in a stoichiometric amount with PsbA2-PSII. Homologous genes to *tll0287* are found in several cyanobacteria. Possible roles for Tll0287 are suggested.

1. Introduction

Light-driven water oxidation catalyzed by Photosystem II (PSII) is the first step in the photosynthetic production of biomass, fossil fuels and O_2 on Earth. Refined three-dimensional X-ray structures from 3.5 Å to 2.9 Å resolution have been obtained using PSII isolated from the thermophilic cyanobacterium *Thermosynechococcus elongatus* [1,2] and at 1.9 Å resolution from *Thermosynechococcus vulcanus* [3]. In *T. elongatus* and *T. vulcanus*, the PSII core complex in which PsbA1 is the D1 protein is made up of 17 trans-membrane proteins (although PsbY is missing in [3]) and 3 extrinsic proteins. The main cofactors involved in the function of PSII are integral components of the D1 (PsbA) and D2 (PsbD) proteins. In total, PSII contains 35 chlorophylls (Chl), 2 pheophytins (Pheo), 2 hemes, 1 non-heme iron, 2 plastoquinones, 3–4 calcium ions, one of which is part of the Mn_4CaO_5 cluster, 3 chloride ions, two of which are at ≈7 Å from the Mn_4CaO_5-cluster, 11–12 carotenoid molecules, more than 20 lipids and ≈1300 water molecules [3].

In PSII, the excitation resulting from the absorption of a photon is transferred to the photochemical trap which undergoes a charge separation. The positive charge is then stabilized on P_{680}, a weakly coupled chlorophyll dimer (P_{D1} and P_{D2}). Then, $P_{680}^{+\bullet}$ oxidizes the tyrosine residue of the D1 polypeptide, Tyr_Z, which in turn oxidizes the Mn_4CaO_5-cluster, the catalytic center for water oxidation. On the acceptor side, the pheophytin anion ($Pheo_{D1}^{-\bullet}$) transfers the electron to the primary quinone electron acceptor, Q_A, which in turn reduces the second quinone, Q_B. Q_A is tightly bound and acts as a one-electron carrier whereas Q_B acts as a two-electron and two-proton acceptor with a stable semiquinone intermediate, $Q_B^{-\bullet}$. While the $Q_B^{-\bullet}$ semiquinone state is tightly bound, the quinone and quinol forms are exchangeable with the quinone pool in the thylakoid membrane, *e.g.* [4–9]. The Mn_4CaO_5-cluster acts both as a complex accumulating oxidizing equivalents and as the catalytic site for water oxidation. The enzyme cycles sequentially through five redox states denoted S_n where *n* stands for

Abbreviations: PSII, Photosystem II; Chl, chlorophyll; MES, 2-(N-morpholino) ethanesulfonic acid; P_{680}, chlorophyll dimer acting as the second electron donor; Q_A, primary quinone acceptor; Q_B, secondary quinone acceptor; 43H, *T. elongatus* strain with a His-tag on the C terminus of CP43; EPR, Electron Paramagnetic Resonance; PQ, plastoquinone 9; CBB, Coomassie Brilliant Blue; PVDF, polyvinylidene fluoride; SDS, sodium dodecyl sulfate; WT*1, WT*2, WT*3, cells containing only the $psbA_1$, $psbA_2$, and $psbA_3$ genes, respectively; $Pheo_{D1}$, pheophytin; P_{D1} and P_{D2}, Chl monomer of P_{680} on the D1 or D2 side, respectively

* Corresponding author. Tel.: 33 1 69 08 72 06; fax: 33 1 69 08 87 17.
** Correspondence to: M. Sugiura, Proteo-Science Research Center, Ehime University, Bunkyo-cho, Matsuyama, Ehime 790-8577, Japan.
E-mail addresses: alain.boussac@cea.fr (A. Boussac), miwa.sugiura@ehime-u.ac.jp (M. Sugiura).

0005-2728/$ – see front matter © 2013 Elsevier B.V. All rights reserved.
http://dx.doi.org/10.1016/j.bbabio.2013.06.002

the number of oxidizing equivalents stored [10,11]. Upon formation of the S_4 state, two molecules of water are rapidly oxidized, the S_0 state is regenerated and O_2 released [5,10–13].

Cyanobacterial species have multiple *psbA* genes encoding the D1 protein, *e.g.* [14–23] which are known to be differentially expressed depending on the environmental conditions, *e.g.* [14–22,24,25]. In particular, specific up/down-regulations of one of these genes under high light conditions are indicative of a photo-protection mechanism. For example, *Synechocystis* PCC 6803, a mesophilic cyanobacterium, has three *psbA* genes in its genome. Two (*psbAII* and *psbAIII*) of these produce an identical D1. Nevertheless, while *psbAII* is expressed under the "normal" laboratory cultivation conditions, transcription of *psbAIII* is induced by high light or UV light [17] and that of *psbAI* seems triggered by micro-aerobic conditions [20]. *T. elongatus* has also three different *psbA* genes in its genome [23]. In this cyanobacterium, it has been reported that $psbA_1$ is constitutively expressed under "normal" laboratory conditions, while the transcription of $psbA_3$ is induced by high light or UV light illumination [18,24,25]. Although it has been demonstrated that transcription of $psbA_2$ is partially induced by microaerobic conditions [20], the essential expression conditions of $psbA_2$ are still not clear.

In *T. elongatus*, among the 344 residues constituting D1 there are 21 substitutions between PsbA1 and PsbA3, 31 between PsbA1 and PsbA2 and 27 between PsbA2 and PsbA3. There are an increasing number of reports aiming at characterizing how the PsbA1/PsbA3 substitution tunes the properties of the PSII cofactors [21,24–30]. The effects of the PsbA(1/3)/PsbA2 substitution are much less documented. In the first study [31], it has been shown that the geometry of the phenol group of Tyr_Z and its environment, likely the hydrogen bond between Tyr_Z and His190, are modified in PsbA2-PSII when compared to PsbA(1/3)-PSII. This previous study also pointed to the dynamics of the proton coupled electron transfer processes associated with the oxidation of Tyr_Z being affected. It was proposed that the Cys144Pro and Pro173Met substitutions in PsbA2-PSII *versus* PsbA(1/3)-PSII, respectively located upstream of the α-helix bearing Tyr_Z and between the 2 α-helices bearing Tyr_Z and its hydrogen-bonded partner, His190, were responsible for these changes.

In this work, by using EPR spectroscopy, absorption spectroscopy, MALDI-TOF/MS spectrometry and biochemical analysis, it is shown that when the *T. elongatus* genome contains only the $psbA_2$ gene encoding D1, a new hemoprotein is present in the non-membrane protein fraction and is also detected associated with the purified PSII core complex.

2. Materials and methods

2.1. T. elongatus strains and isolation of PSII complexes

The constructions of *psbA*-deletion mutants from a *T. elongatus* 43-H strain that had a His_6-tag on the C-terminus of CP43 [32] and that had only either the $psbA_1$ gene (WT*1) [29] or the $psbA_2$ gene (WT*2) [31] or the $psbA_3$ gene (WT*3) [33] have been described previously. The cells were grown in 1-L cultures of DTN in 3-L Erlenmeyer flasks in a rotary shaker with a CO_2-enriched atmosphere at 45 °C under continuous light (Grolux, Sylvania) as previously described [31–33]. After the breaking of the cells with a French press the unbroken cells were pelleted by centrifugation for 5 min at 3000 *g*. Then, the thylakoid membranes were pelleted by ultracentrifugation for 25 min at 300,000 *g*. Before the addition of the detergent to the thylakoids they were extensively washed (by resuspension/centrifugation cycles) until the supernatant became clear, *i.e.* almost free from non-membrane proteins. The supernatants containing the non-membrane proteins were frozen at −28 °C until used. The PSII core complexes were then prepared essentially as described earlier [31–33]. For PSII purification, glycerol was avoided from the elution step of the Ni^{2+}-column to the end of the purification. The final resuspending medium for PSII contained 1 M betaine, 15 mM $CaCl_2$, 15 mM $MgCl_2$, 40 mM MES, pH 6.5 (adjusted with NaOH).

For the $CaCl_2$-washing treatment, the PSII was first pelleted by centrifugation for 3 h at 600,000 *g*. Then, the pellet was resuspended in 2 M $CaCl_2$ and incubated for 30 min on ice. Then, the PSII was again pelleted by centrifugation for 3 h at 600,000 *g* before resuspension in 1 M betaine, 15 mM $CaCl_2$, 15 mM $MgCl_2$, 40 mM MES, pH 6.5. The supernatant containing the proteins released by the $CaCl_2$-washing was concentrated by using Amicon Ultra-15 concentrator devices (Millipore) with a 3 kDa cut-off. Two to three cycles of concentration/dilution in 1 M betaine, 15 mM $CaCl_2$, 15 mM $MgCl_2$, 40 mM MES, pH 6.5 were repeated before freezing the samples at −28 °C. Tris-washing was done as the $CaCl_2$-washing but with 1.2 M Tris, pH 9.2. Absorption spectra were recorded with a Uvikon XL spectrometer.

2.2. EPR spectroscopy

Cw-EPR spectra were recorded using a standard ER 4102 (Bruker) X-band resonator with a Bruker Elexsys 500 X-band spectrometer equipped with an Oxford Instruments cryostat (ESR 900). The PSII samples at ≈1.6 mg of Chl mL^{-1} were loaded in the dark into quartz EPR tubes and further dark-adapted for 1 h at room temperature. Then, the samples were frozen in the dark to 198 K and then transferred to 77 K in liquid N_2. The samples containing the proteins released by the $CaCl_2$-washing treatment and the samples containing the soluble proteins of the cells were loaded into quartz EPR tubes and they were frozen to 198 K and then transferred to 77 K. Prior to the measurements all the samples were degassed at 198 K.

2.3. MALDI-TOF/mass spectroscopy

MALDI-TOF/MS measurements were done as described earlier [27,34]. The isolated PSII complexes (30 and 150 μg of Chl mL^{-1} for linear mode and reflector mode, respectively) were mixed with the same volume of a saturated matrix (sinapic acid, Fluka) solution that consisted of 60% acetonitrile and 0.1% trifluoroacetic acid. MALDI-TOF mass analysis was performed using a Voyager-DE PRO MALDI-TOF mass spectrometer (Applied Biosystems). The instrument was operated in reflector mode at a 20-kV accelerating voltage and 100-ns ion extraction delay with the nitrogen laser working at 337 nm and 3 Hz. Two hundred laser flashes were accumulated per spectrum. The m/z values in Fig. 4 result from the average of hundred spectra. Internal calibration was performed on the samples premixed with human adrenocorticotropic hormone fragment (from Sigma, average $m/z = 2466.72$, resolved $m/z = 2465.1989$), with bovine insulin (from Sigma, average $m/z = 5734.51$, resolved $m/z = 5730.6087$) and bovine heart apomyoglobin (from Sigma, average $m/z = 16952.27$).

2.4. SDS-polyacrylamide gel electrophoresis

PSII complexes were solubilized with 2% lithium lauryl sulfate and then analyzed by SDS-polyacrylamide gel electrophoresis with a 16–22% gradient gel containing 7.5 M urea as described previously [35].

2.5. Determination of N-terminal sequence

After the SDS-polyacrylamide gel electrophoresis, protein bands were transblotted onto PVDF membrane (Amersham Hybond-P, GE Healthcare). Then, the proteins were stained with Coomassie Brilliant Blue (CBB). The N-terminal sequencing of the band cut from the PVDF membrane was done by the Edman procedure (Genosphere Biotech., Paris).

2.6. Mascot after tryptic digestion and MALDI-MS/MS

Proteins released from PSII by $CaCl_2$ washing and the extra band in PsbA2-PSII in Fig. 2 were both analyzed by this technique (SIMOPRO, CEA Saclay).

2.7. Gel filtration chromatography

PSII samples (50 μL at 0.5 mg Chl mL^{-1}) in 40 mM MES, 15 mM $MgCl_2$, 15 mM $CaCl_2$, 100 mM NaCl and 0.03% β-DM at pH 6.5 were loaded on a BioSep-SEC-S 3000 column mounted on a BioLogic Duo Flow System (Bio-Rad) with Quad Tec™ UV/VIS detector (Bio-Rad) for detection of both absorption at 280 nm and 673 nm. The flow rate was set up to 1 mL min^{-1} with the same buffer as above. Fractions of 0.5 mL were successively collected. The working pressure was about 600 psi.

3. Results

Fig. 1 shows the EPR spectra recorded on the fractions containing all the non-membrane proteins obtained after the breaking of the cells and the removal of the membranes by centrifugation. Spectrum a was recorded on the soluble proteins from WT*1 cells, spectrum b on the soluble proteins from WT*2 and spectrum c on the soluble proteins from WT*3 cells. In the three samples, among the easily EPR detectable species, there were the Cytc_{550} pool exhibiting a g_z value at 2.96 (≈2290 G) [36] and the Fe-superoxide dismutase pool with characteristic resonances below 2000 G [37]. The resonance at ≈2700 G ($g \approx 2.51$) likely corresponded to the g_z resonance of the proportion of Cytc_6 which was oxidized under these conditions. The six lines centered at $g = 2$ arose from free Mn^{2+}.

From the experiment reported in Fig. 1 an additional EPR signal with the characteristic shape of an oxidized low spin cytochrome with $g_z = 2.41$ and $g_x = 1.91$ was detected in the non-membrane proteins extracted from WT*2 cells. The g_y value could not be determined accurately here because it is superimposed on the g_y signal from other cytochromes but as it will be shown below is close to 2.24. To see if the protein content of purified PSII was also affected by the presence of PsbA2 we have compared the purified PsbA2-PSII to PsbA1-PSII and PsbA3-PSII.

Comparison of the polypeptide content of purified PsbA2-PSII with that of PsbA1-PSII and PsbA3-PSII was done by SDS-polyacrylamide gel electrophoresis and MALDI-TOF mass spectrometry. The CBB-staining after the SDS-polyacrylamide gel electrophoresis is shown in Fig. 2. It allows us to visualize the protein content in the molecular mass range from ≈8 kDa to ≈50 kDa. The major change observed in Fig. 2 was the presence of a band at ≈19 kDa (indicated with an asterisk) in PsbA2-PSII which was not detected in PsbA1-PSII and PsbA3-PSII. The migration of the D1 protein (PsbA2) was also found slightly but reproducibly faster in PsbA2-PSII than in both PsbA1-PSII and PsbA3-PSII. This was confirmed by an immuno-blot analysis with an antibody against D1 and used on purified PsbA2-PSII (see Supplementary material). In contrast, the immunoblot analysis performed with thylakoids did not reveal any differences in the migration of the D1 protein in none of the 3 samples. Since under saturating continuous illumination the oxygen evolving activity of purified PsbA2-PSII was found similar to that of PsbA1-PSII [31], it seems unlikely that a D1 degradation was at the origin of the slightly different migration observed in PsbA2-PSII. A better characterization of this (these) change(s) will be the subject of future works.

Because the separation of small peptides with a molecular mass smaller than 10 kDa is difficult on a gel electrophoresis, purified PSII was also analyzed with MALDI-TOF mass spectrometry (Fig. 3). The polypeptide contents of the PsbA1-PSII, PsbA2-PSII and PsbA3-PSII complexes in the low m/z ranges from 3800 to 5200 and 5500 to 18,000 are shown in Fig. 3A and B, respectively. Fig. 3A shows that the content of the small peptides, PsbT, formylated PsbM (M-for), PsbJ, acetylated PsbM (M-ace), PsbK, PsbX, PsbL, PsbI, PsbY, PsbF and Psb30 in PsbA2-PSII (spectrum b) was similar to that in PsbA1-PSII (spectrum a) and to that in PsbA3-PSII (spectrum c). In the m/z range from 5500 to 18,000, Fig. 3B, the PsbZ, PsbH, PsbE, PsbU and PsbV peptides were

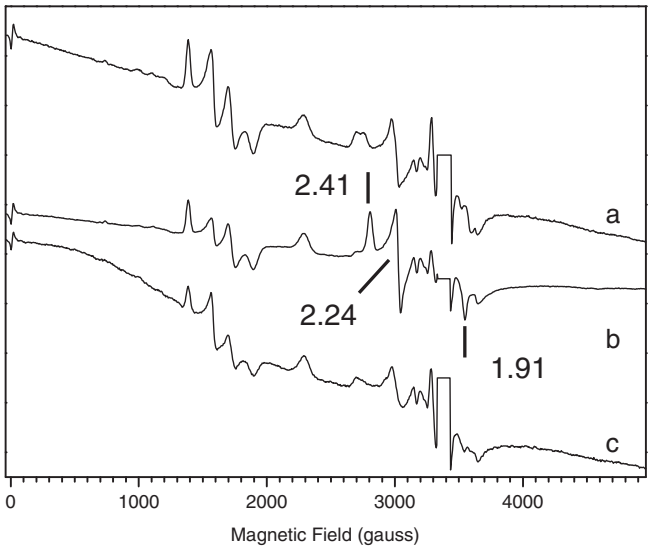

Fig. 1. Comparison of the EPR spectra recorded on the supernatant of the membrane containing fraction after the breaking of WT*1 cells (a), WT*2 cells (b) and WT*3 cells (c). The spectra were arbitrarily scaled to the amplitude of the g_z signal of Cytc_{550}. Instrument settings: modulation amplitude, 25 G; microwave power, 20 mW; temperature, 30 K; microwave frequency, 9.4 GHz; modulation frequency, 100 kHz.

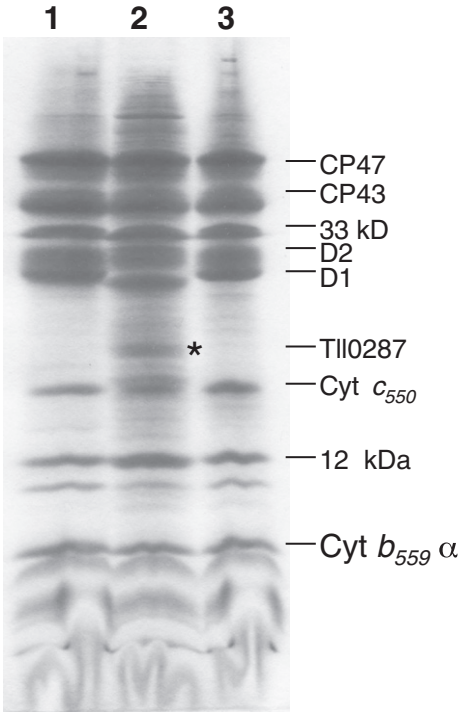

Fig. 2. CBB-staining of SDS-polyacrylamide gel electrophoresis of isolated PsbA1-PSII (lane 1), PsbA2-PSII (lane 2) and PsbA3-PSII (lane 3). The amount of PSII loaded was 8 μg of Chl. An asterisk shows the extra protein band around 19 kDa. The number on the left indicates the molecular masse scale in kDa. The CP47 is PsbB, the CP43 is PsbC, the 33 kDa protein is PsbO, D2 is PsbD, D1 is PsbA, Cytc_{550} is PsbV, the 12 kDa protein is PsbU, Cytb_{559} α is PsbE.

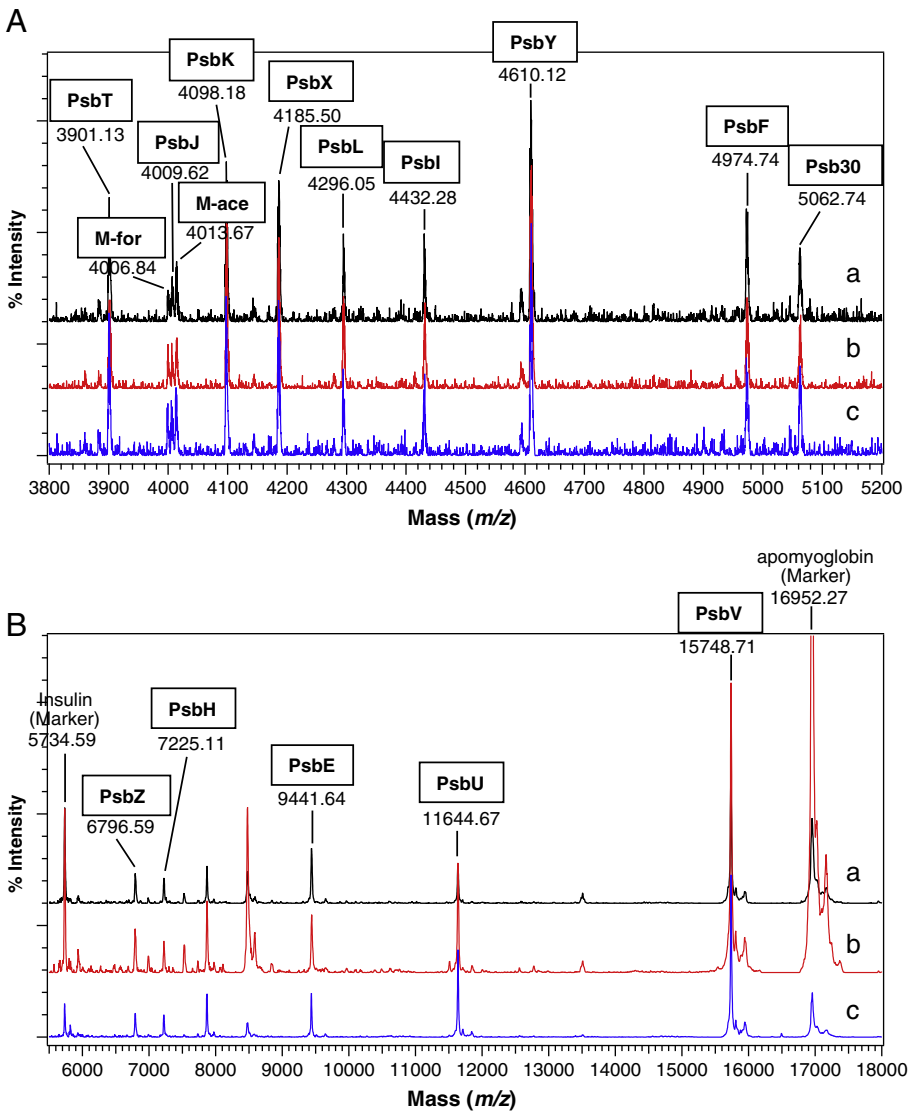

Fig. 3. MALDI-TOF mass spectra in m/z 3800–18,000 molecular mass range of isolated PsbA1-PSII (a), PsbA2-PSII (b) and PsbA3-PSII (c) in the reflector mode (panel A) from m/z = 3800 to 5200, and in the linear mode (panel B) from m/z = 5500 to 18,000. Numbers under annotations indicate m/z values. Human adrenocorticotropic hormone fragment with m/z = 2465.1989 and bovine insulin m/z = 5730.6087 were used to calibrate the m/z scale in reflector mode (panel A). In linear mode (panel B), bovine insulin with m/z = 5734.59 and bovine heart apomyoglobin with m/z = 16,952.27 were used for the calibration. The unlabeled peaks at m/z = 7874 and m/z = 8476 very likely correspond to PsbV and apomyoglobin, respectively, for z = 2.

detected to the same extent in the three PSII complexes. The PsbE (the α subunit of Cytb_{559}), PsbU (the extrinsic 12 kDa protein) and PsbV (the Cytc_{550}) were also clearly detected in the SDS-polyacrylamide gel electrophoresis. So, there were no additional peptides and no missing peptides in any of the 3 PSII core complexes in the 3800 Da to 18,000 Da range (Fig. 3) and in the high molecular mass range (Fig. 2) with the exception of the ≈19 kDa protein present in PsbA2-PSII. The peptides detected here in PsbA1-PSII were those and only those present in the X-ray structure. Accordingly, the purification procedures resulted in PSII free from major contaminations detectable by MALDI-TOF mass spectrometry.

To better estimate the molecular mass of the new protein(s) detected in lane 2 of Fig. 2, the MALDI-TOF spectra were recorded in the m/z region between 14,000 and 20,000 (Fig. 4). Spectrum a was recorded on PsbA1-PSII, spectrum b on PsbA2-PSII and spectrum c on PsbA3-PSII. As expected from Fig. 2, extra protein(s) was (were) found in the m/z region around 19,000 Da in PsbA2-PSII. Several peaks were observed and to estimate accurately the molecular size of each of them, a hundred of experiments were averaged in spectrum b. The molecular masses of these new proteins detected in PsbA2-PSII were found to be 18,616.43 Da, 18,983.43 Da, 19,147.98 Da, 19,165.73 Da and 19,842.55 Da. In the following we present the results of experiments aiming at identifying these new proteins.

The amino acid sequence(s) of the new protein(s) was (were) analyzed by two different methods. First, the extra band at ≈19 kDa on the SDS-polyacrylamide gel electrophoresis in Fig. 2 was analyzed with a N-terminal sequencing procedure by using the Edman degradation. N-terminal sequences corresponding to SANPE, APLAS, ASLWI and possibly GSPAP were found (see Supplementary material). A BLAST search indicated that all these sequences belong to the *tll0287* gene product in *T. elongatus*. This was further confirmed with Mascott after tryptic digestion and MALDI-MS/MS analysis (see Supplementary material). Until now the *tll0287* gene product was registered as a hypothetical protein with an unknown function. The protein sequence deduced from the *tll0287* gene is shown in Fig. 5.

Fig. 6 shows the EPR spectra of purified PsbA2-PSII recorded with a microwave power equal to 20 mW at either 8.6 K (spectrum a) or 30 K (spectrum b). Signals at magnetic field values lower than

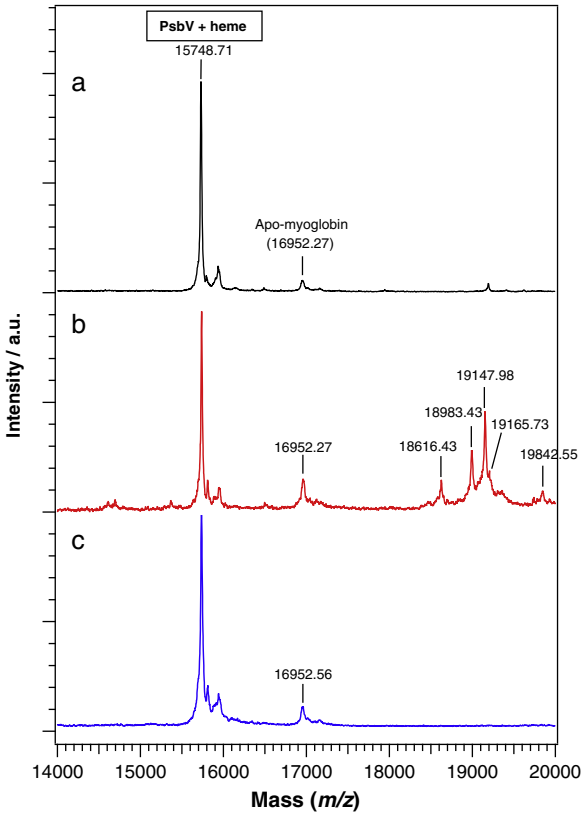

Fig. 4. MALDI-TOF mass spectra in the 14,000–20,000 molecular mass range of isolated PsbA1-PSII (a), PsbA2-PSII (b) and PsbA3-PSII (c) in the linear mode.

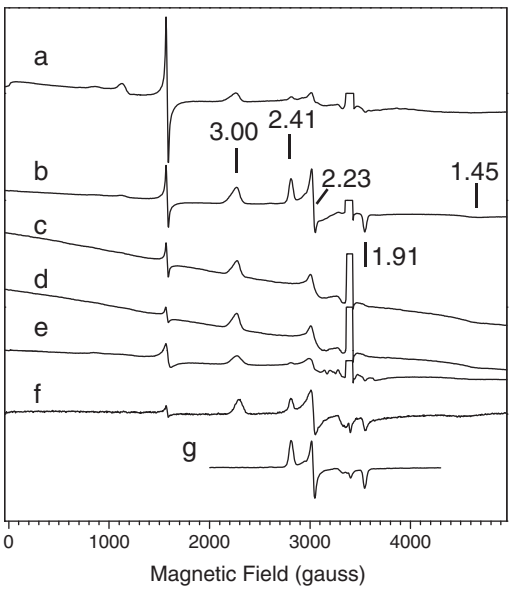

Fig. 6. EPR measurements: Spectrum a, untreated PsbA2-PSII at 8.6 K. Spectrum b, untreated PsbA2-PSII at 30 K; Spectrum c, untreated PsbA1-PSII at 30 K; Spectrum d, untreated PsbA3-PSII at 30 K. Spectrum e, $CaCl_2$-washed PsbA2-PSII at 30 K. Spectrum f, supernatant of the $CaCl_2$-washing of PsbA2-PSII at 30 K; Spectrum g partially purified Tll0287 protein at 30 K. Other instrument settings: modulation amplitude, 25 G; microwave power, 20 mW; microwave frequency, 9.4 GHz; modulation frequency, 100 kHz. For spectra a, b and c [Chl] was 1.6 mg mL^{-1} and the $Tyr_D^{\bullet}$ spectral region at $g \approx 2$ was deleted. The amplitude of spectrum g was arbitrarily scaled.

1600 G arise from high spin Fe^{3+} species and signals at $g = 3.00$ and $g = 1.45$ arise from $Cytc_{550}$ and from $Cytb_{559}$ in centers in which this cytochrome was oxidized. All these signals were detected at both 8.6 K and 30 K. In contrast, increasing the temperature from 8.6 K to 30 K strongly enhanced the amplitude of a new signal, detected as a trace in spectrum a, with a positive feature at $g = 2.41$ and a negative one at $g = 1.91$. The resonances at $g = 2.41$ and $g = 1.91$ are identical to those detected in spectrum b in Fig. 1 and were detected neither in PsbA1-PSII (spectrum c) nor in PsbA3-PSII (spectrum d). They very likely originate from the newly identified proteins in Fig. 2 and 4. So, the Tll0287 protein found in a large amount in the fraction containing the non-membrane proteins was also found associated to the purified PsbA2-PSII. Fig. 7 shows the EPR spectra recorded in extensively washed thylakoids (spectrum a) and in purified PsbA2-PSII (spectrum b). The ratios $Tll0287_{(PSII\ bound)}/Cytc_{550(PSII\ bound)}$ in membranes before the addition of the detergent and in purified PSII were found similar. The dimer and monomer forms of PSII were also further purified by gel filtration chromatography (not shown). SDS-polyacrylamide gel electrophoresis analysis revealed that both the dimer and monomer forms retained some Tll0287 protein. All these observations argue against a contamination. Rather, they suggest that Tll0287 is associated to the PSII core complex when D1 is PsbA2. Indeed, a contamination is expected to disappear during the PSII purification from thylakoids and the further gel filtration chromatography.

The new EPR signal from Tll0287 detected here was not observed in the first study of PsbA2-PSII [31] in which the EPR spectra were recorded at 8.6 K and at 20 mW for the microwave power. The microwave power saturation characteristics of the new species were therefore more precisely determined in the experiment reported in Fig. 8 and they were compared to those of $Cytc_{550}$ and $Cytb_{559}$. Fig. 8 shows the microwave power saturation characteristics of the new g_z resonance at $g = 2.41$ (triangles), of the g_z resonance of $Cytc_{550}$ at $g = 3.0$ (squares) and of the g_z resonance ($g = 3.07$) of the

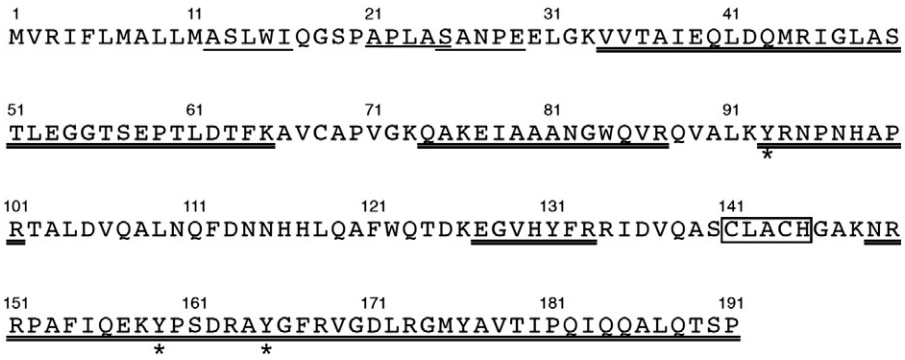

Fig. 5. Deduced amino acid sequence from the *tll0287* gene in *T. elongatus*. The underlined amino acid residues are those belonging to the main N-terminal sequences detected by using the Edman procedure. The frame shows the conserved heme-binding motif (CxxCH) and the stars the conserved tyrosine residues which are potential candidates to be the 6th heme iron axial ligand. The doubly underlined amino acids are those belonging to the fragments identified with Mascot after tryptic digestion and MALDI-MS/MS.

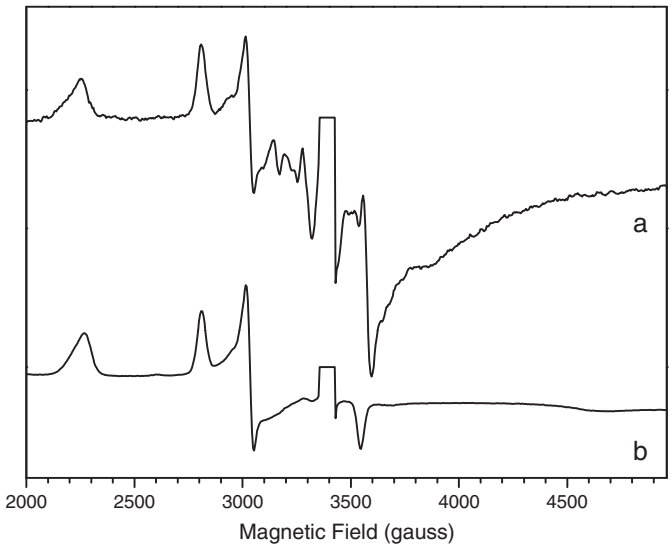

Fig. 7. Comparison of the EPR spectra recorded with PsbA2-thylakoids (a) and with PsbA2-PSII. The two spectra were scaled to the amplitude of the g_z signal of Cytc_{550}. Same instrument settings as in Fig. 6.

non-relaxed state of the high potential form of Cytb_{559} in the same untreated PsbA2-PSII sample (circles). This latter signal was induced by 77 K illumination after the recording of the two previous sets of data. Data were collected at 15 K. The continuous lines correspond to the fits of the experimental data points using the equation: Signal amplitude $= k\sqrt{P} / (1 + P / P_{1/2})^{b/2}$ with k a proportionality factor, P the applied microwave power, $P_{1/2}$ the microwave power at half-saturation and b the inhomogeneity factor. The $P_{1/2}$ and b parameters were respectively found to be equal to 76 mW and 2.2 for Cytb_{559}, 11 mW and 1.4 for Cytc_{550}, and 2.1 mW and 1.5 for the $g_z = 2.41$ resonance. Clearly, the g_z resonance at $g = 2.41$ saturates at a lower microwave power than that from Cytc_{550} and at an even much lower microwave power than the g_z resonance from Cytb_{559}. The tendency of the $g_z = 2.41$ resonance to strongly saturate under

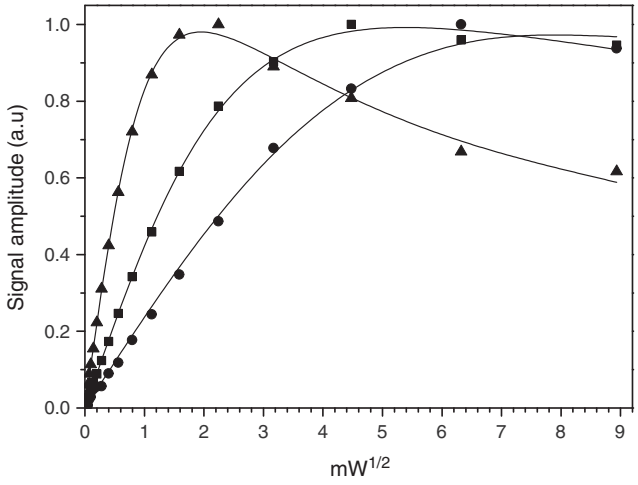

Fig. 8. Amplitude of the g_z resonance at 15 K *versus* the square root of the microwave power for Cytc_{550} (squares) and for the non-relaxed state of the high potential form of Cytb_{559} induced by 77 K illumination ($g_z = 3.07$) in the same untreated PsbA2-PSII sample (circles) and for the new resonance at $g_z = 2.41$ (triangles). The continuous lines correspond to the fit of the experimental data points using the equation: Signal amplitude $= k\sqrt{P} / (1 + P / P_{1/2})^{b/2}$ with k a proportionality factor, P the applied microwave power, $P_{1/2}$ the microwave power at half-saturation and b the inhomogeneity factor. The $P_{1/2}$ and b parameters were respectively found to be equal to 76 mW and 2.2 for Cytb_{559}, 11 mW and 1.4 for Cytc_{550}, and 2.1 mW and 1.5 for the new $g_z = 2.41$ resonance.

the microwave power conditions used to record the S_2 multiline signal explains why this signal could escape detection in our previous work [31]. These relaxation properties also suggest that either the distance between the newly identified heme and potentially relaxing species like paramagnetic metals present in PSII or the spin lattice relaxation properties strongly differ when compared to Cytc_{550} and Cytb_{559}.

In an attempt to purify the new protein, biochemical treatments known to release the extrinsic proteins from PSII have been tested. Such treatments were done on PsbA2-PSII first pelleted by ultracentrifugation. Then, both a $CaCl_2$-washing and a Tris-washing were found effective in the release of the protein exhibiting the new EPR signals in addition to the release of the PsbV (Cytc_{550}), PsbU (12 kDa) and PsbO (33 kDa) proteins (not shown). Spectrum e in Fig. 6 was recorded on $CaCl_2$-treated PsbA2-PSII pelleted by centrifugation and spectrum f was recorded on the supernatant of the $CaCl_2$-washing procedure. In spectrum e, the signal from Cytc_{550} greatly decreased and that one with $g_z = 2.41$ and $g_x = 1.91$ fully disappeared. The signal at $g \approx 3.0$ results now from the superimposition of the g_z resonance of the still PSII bound Cytc_{550} to the g_z resonance of Cytb_{559} which was converted into the low potential form by the treatment and which was oxidized at the ambient potential. Spectrum f shows slightly modified g values for the unbound Cytc_{550} as previously reported [36]. Resonances at $g = 2.41$ and $g = 1.91$ were now detected in the sample containing the proteins released by the $CaCl_2$-treatment. From the comparison of spectra b and d in Fig. 6 it is clear that the new heme protein exhibited similar g_z and g_x values in the unbound and bound states in contrast with Cytc_{550} which exhibits a small change in the g values in the unbound and bound states [36].

A gel permeation chromatography has been performed on the fraction containing the proteins released by either Tris-washing or $CaCl_2$-washing. The absorption spectrum of the partially purified Tll0287 protein shows that it was mainly oxidized and that the Soret band was at 415 nm instead of 407 nm for Cytc_{550} (see Supplementary material). Spectrum g in Fig. 6 was recorded on the fraction from the gel permeation enriched in the Tll0287 protein and lacking the Cytc_{550}. The EPR signal was similar to that recorded in purified PsbA2-PSII (spectrum b). From spectrum g, the g_y value of the Tll0287 protein could also be determined to be 2.24.

Fig. 9 shows a MALDI-TOF analysis of the pellet (spectrum b) and of the supernatant (spectrum c) resulting from the $CaCl_2$-treatment on PsbA2-PSII. These two samples exhibit the EPR spectra e and f, respectively, in Fig. 6. For an easier comparison, spectrum a in Fig. 8 corresponds to untreated PsbA2-PSII and is a re-plot of spectrum b in Fig. 4. In spectrum b of Fig. 9, the signal from Cytc_{550} greatly diminished, the mass if with $m/z \approx 19{,}000$ fully disappeared in $CaCl_2$-treated PSII and the released proteins appeared in the supernatant (spectrum c). Consistently with the EPR data, the $CaCl_2$-washing resulted in the removal of Cytc_{550} bound to PSII (the PsbV containing heme with $m/z \approx 15{,}748$) in the great majority of centers and in the total removal of proteins with peaks with m/z values between 18,000 and 20,000. So, one or some of these peptides bind a heme and as it will be shown below, it seems likely that the peak at m/z 19,147.98 in spectrum a is very likely equivalent to the peak at m/z 19,150.34 in spectrum c.

From the experiments reported in Fig. 4 and 9, and from the N-terminal sequencing, the Tll0287 protein could be detectable with different sizes. Table 1 summarized the calculated and experimentally determined molecular masses of Tll0287 with tentative correspondences between the different peaks in the MALDI-TOF spectra and the different N-terminal sequences found. The polypeptides with m/z values equal to 18,616.43, 18,983.43, 19,147.98 and 19,842.55 observed in the MALDI-TOF/MS very likely correspond to truncated polypeptides after positions 24, 20, 17 and 11, respectively. The peak at m/z 19165.73 could correspond to the peptide with 24 residues truncated on the N-terminal region (Δ24) and with the heme bound. In conclusion, all polypeptides detected around 19 kDa in the MALDI/TOF mass

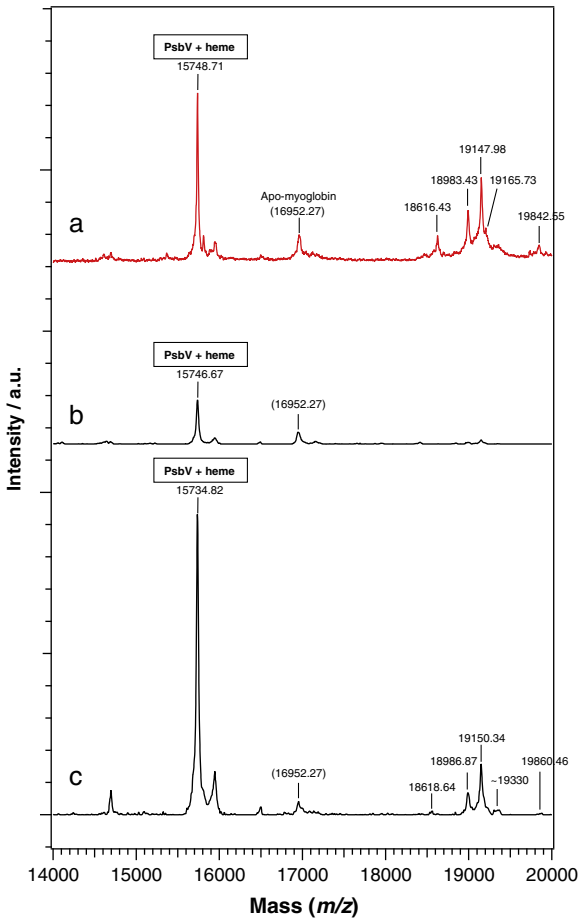

Fig. 9. Comparison by MALDI-TOF mass spectra in the 14,000–20,000 molecular mass range between untreated PsbA2-PSII (spectrum a), pellet of $CaCl_2$ washed PsbA2-PSII (spectrum b) and supernatant of $CaCl_2$-washed PSII containing the proteins released by the treatment (spectrum c).

spectra originate from only one protein species. The *tll0287* gene product seems to be detectable with at 4 N-terminal sequences that are: SANPE, APLAS, GSPAP and ASLWI. For the proteins with APLAS and SANPE for the N-terminal sequences, an extra mass around 70–80 Da was detected. The origin of this extra mass remains to be determined but could originate from a heme fragment bound to the protein after a partial degradation of the heme during the MALDI-TOF experiment.

Table 1
Calculated and experimentally determined molecular masses of the Tll0287 protein with the different N-terminal sequences found by using the Edman procedure.

N-ter sequence	Processing site (truncation)	Calculated mass $[M+H]^+$ in Da		Experimentally measured mass $[M+H]^+$ in Da	
		−Heme	+Heme[a]	−Heme	+Heme
ASLWI	11/12(Δ11)	19838.16	20456.37	19842.55[b] (+4.00)[c]	nd[d]
GSPAP	17/18(Δ17)	19139.35	19757.56	19147.98[b] (+8.63)[c]	nd[d]
APLAS	20/21(Δ20)	18898.11	19516.32	18983.43[b] (+85.32)[c]	nd[d]
				18964.81[e] (+66.70)[c]	
SANPE	24/25(Δ24)	18545.68	19163.89	18616.43[b] (+70.75)[c]	19165.73[e] (−1.84)[c]

[a] The increase of the molecular mass due to the binding of the heme was experimentally found in this work to be 618.70 Da for $Cytc_{550}$.
[b] Intact PSII.
[c] Difference between the calculated average molecular mass and the experimental value.
[d] nd = not detected.
[e] Supernatant of the $CaCl_2$-washing.

4. Discussion

In addition to the 20 proteins found in the crystals of PSII, other proteins like Psb27, *e.g.* [38–41], Psb28, *e.g.* [39–42], Psb29 [43], PsbP (or CyanoP) and PsbQ (or CyanoQ) *e.g.* [38–41], and Ycf48 *e.g.* [43] were found to be present in a proportions of PSII centers under certain conditions. Some of these proteins have been proposed to be involved in repair processes, assembly processes and PSII function, *e.g.* [39–45]. The 3D structures of CyanoP [46], Psb27 [47] and Psb28 [48] have been recently determined.

Here, we show that a new protein is associated to PsbA2-PSII in *T. elongatus* WT*2 cells in which both $psbA_1$ and $psbA_3$ are deleted and therefore with PsbA2 as the D1 protein. This new protein was detected neither in PsbA1-PSII nor in PsbA3-PSII [33,49]. EPR measurements showed that this is a heme containing protein. The results of the sequencings allowed us to identify this new protein to be the product of the *tll0287* gene. Until now the *tll0287* gene product has been registered in the cyanobase (http://genome.kasuza.or.jp/cyanobase/thermo) as a hypothetical protein with an unknown function. Genes potentially coding for a homologous hemoprotein are present in several cyanobacteria (see Supplementary material).

An incidental co-purification of the Tll0287 present in the non-membrane protein with PsbA2-PSII or an unspecific binding to the PSII cannot be totally discarded. However we do not favor this hypothesis for the following reasons: First, before the addition of the detergent to the membranes these ones were extensively washed (by resuspension/centrifugation cycles) until the supernatant became clear. Second, an ultracentrifugation of the PsbA2-PSII did not modify significantly the Tll0287 content in PSII. Third, a washing with a high concentration of salt ($CaCl_2$, 2 M) or Tris (1.2 M, pH 9.2) was required to separate the Tll0287 protein from the purified PSII. Fourth, we have estimated by EPR the ratio $Tll0287_{(PSII\ bound)}/Cytc_{550(PSII\ bound)}$ in membranes before the addition of the detergent and in purified PSII. The two ratios were similar. Fifth, both the PSII monomer and PSII dimer further purified by gel filtration chromatography retained some Tll0287 protein. All these five points argue against a contamination. So, the presence of a large pool of the Tll0287 protein in whole WT*2 cells and the association of this protein to PsbA2-PSII very likely appear as a consequence of the presence of PsbA2 as the D1 protein. It should be noted, however, that Tll0287 was detected at a trace level in WT*1 cells (Fig. 4).

From the X-ray crystal structure of $Cytc_{550}$ with a 1.9 Å resolution when bound to PSII [3] and from the 1.8 Å resolution structure of $Cytc_{550}$ in the unbound state [36], we know that the heme of this cytochrome is not subject to chemical modifications after the covalent binding to the 2 cysteine residues (Cys37 and Cys40). Consistently, the difference between the calculated average molecular mass of the apo-$Cytc_{550}$ without the transit peptide (15,130.01 Da) and the experimentally detected molecular mass of the mature $Cytc_{550}$ (m/z = 15,748.71 in Fig. 4, spectrum a) could be estimated to 618.70 Da, *i.e.* very close to the molecular mass of the heme (616 Da). This identity shows that we can rely on the molecular masses experimentally determined by MALDI-TOF/MS in this m/z range. From the MALDI-TOF analysis and the N-terminal sequencing we found at least 4 differently truncated Tll0287 proteins bound to PsbA2-PSII. As summarized in Table 1, the Tll0287 protein had 11 truncated amino acid residues (Δ11; ASLWI…), 17 truncated residues (Δ17; GSPAP…), 20 truncated residues (Δ20; APLAS…) and 24 truncated residues (Δ24; SANPE…) in the N-terminal region. A form with m/z = 19,165.73 which corresponds to the molecular mass of Δ24-Tll0287 with a heme bound was also detected. However, no peptide with a molecular mass corresponding to the 3 other truncated Tll0287 with a heme bound was detected. These results suggest that Tll0287 could be gradually digested on the N-terminal region and that the polypeptide binds a heme when 24 residues are digested. The mature Tll0287 protein seems to be very likely the Δ24 form. The reasons and the process of this maturation process

would have to be clarified in future. The lack of several amino acids on the N-terminal region of the PSII bound Tll0287 protein suggests that the lacking amino acids belong to the transit peptide and therefore that the protein is located on the lumenal side.

From the intensity of the extra band in the SDS-polyacrylamide gel electrophoresis the Tll0287 protein seems associated to a large proportion of purified PsbA2-PSII. However, from the MALDI-TOF mass spectrometry discussed above, only the Tll0287 form with the SANPE N-terminal sequence is expected to bind a heme. In agreement with that, the amplitude of the Tll0287 EPR signal indicates a substoichiometric amount if we assume that the heme was fully oxidized. Indeed, the Tll0287 EPR signal is more narrow than the Cytc_{550} EPR signal and for a same spin concentration the amplitude of the g_z resonance of Tll0287 should be roughly 8 fold larger than that of Cytc_{550} (not shown) when both spectra are recorded under non-saturating microwave conditions (*i.e.* with less than 1 mW at 15 K from Fig. 8). Although Tll0287 seems almost stoichiometrically associated with PsbA2-PSII from SDS-polyacrylamide gel electrophoresis, from the spectra in Fig. 6 and 7 the heme-containing Tll0287 protein corresponds to approximately 25% of the Cytc_{550} content. We have observed that the amplitude of EPR signal from Tll0287 could slightly vary from PSII preparation to PSII preparation. However, the ratio Tll0287$_{(\text{PSII bound})}$/Cyt$c_{550(\text{PSII bound})}$ was found similar in thylakoids and purified PSII. This indicates that the amount of Tll0287 associated to PSII likely results from a process which depends on the culture conditions. Experiments are under progress to find which parameter is involved in such a regulation of the PSII-bound level of Tll0287. This situation looks like that of Psb27, Psb28, Psb29, CyanoP, CyanoQ and Ycf48 which are bound to PSII under certain conditions (see above).

For Cytc_{550} a correlation has been done between the heme-axial ligands' geometry and the rhombicity calculated from the *g* values [36]. This correlation indicated that the binding of Cytc_{550} to PSII was likely accompanied by structural changes in the heme vicinity with a more distorted heme/axial ligand geometry [50–52] when bound to PSII. Indeed, by comparing the crystal structure at 1.8 Å resolution of the isolated Cytc_{550} [36] with that at 1.9 Å resolution of the Cytc_{550} bound to PSII [3] it appears that the heme/axial ligand geometry is more distorted when Cytc_{550} is bound to PSII (not shown but see Supplementary material). For the Tll0287 protein, the rhombicity parameter, $v/\Delta = 0.93$, and the tetragonality parameter, $\Delta/\lambda = 5.27$, suggest that the 2 heme axial ligands are likely His and Tyr. In addition to the conserved CxxCH motif, the absence of a second conserved His residue and the presence of 3 conserved Tyr residues (Fig. 5) argue in favor of Tyr as a potential candidate to be the 6th heme iron axial ligand. A tyrosine for the 6th axial ligand is not a common structure. Among the rare cases we can cite for example the six-coordinate low-spin form of MauG involved in the posttranslational modifications of methylamine dehydrogenase *e.g.* [53] and references therein, the CCmE protein [54] involved in Cyt*c* maturation, *e.g.* [55], the Cyt*cd1* nitrite reductase [56], the hemophore HasA belonging to a heme acquisition system, *e.g.* [57]. The EPR data and the UV–visible absorption spectrum of the partially purified Tll0287 protein indicate that it is mainly in an oxidized state consistently with a Tyr ligation expected to result in a low potential heme. Coincidentally, the molecular mass of the Tll0287 protein, which is relatively high for a soluble hemoprotein when compared to the other cytochromes involved in electron transfer reactions is close to HasA which exists in two forms, a membrane bound and a free form.

It is striking to find a variety of N-terminal sequences for Tll0287. Since the "SLWIQGSPAPLASANPE" sequence of Tll0287 corresponds to a poor PEST sequence [58], we can wonder if this variety has a physiological meaning in possibly a kind of heme transfer or a sort of Cyt*c* maturation system, *e.g.* [55,59–61] for reviews on the different Cyt*c* maturation systems. Alternatively, since the expression of the *psbA2* gene has been shown to occur under micro-aerobic conditions [18], in the presence of ≈20% O_2 the production of Tll0287 in WT*2 cells could be the answer to an oxidative stress. Future works would have to solve these questions. In particular, a proteomic study aiming at identifying other proteins co-expressed with Tll0287 has been undertaken. Interestingly, spectrum a in Fig. 4 shows that a very small amount of the Tll0287 protein was found bound to PsbA1-PSII. This suggests that the mechanism requiring the association of Tll0287 to PSII could be a general mechanism but, in the PsbA2-PSII case, the step resulting in the dissociation/degradation of a PSII-Tll0287 complex is a limiting step.

Acknowledgements

B. Lagoutte, A. Desbois and D. Picot are acknowledged for their discussions. V. Mary is acknowledged for technical help. MS was supported by the JST-PRESTO program (4018). AB was supported in part by a CEA/DSV "Bioénergie" grant.

Appendix A. Supplementary data

Supplementary data to this article can be found online at http://dx.doi.org/10.1016/j.bbabio.2013.06.002.

References

[1] K.N. Ferreira, T.M. Iverson, K. Maghlaoui, J. Barber, S. Iwata, Architecture of the photosynthetic oxygen-evolving center, Science 303 (2004) 1831–1838.
[2] A. Guskov, J. Kern, A. Gabdulkhakov, M. Broser, A. Zouni, W. Saenger, Cyanobacterial photosystem II at 2.9-Å resolution and the role of quinones, lipids, channels, and chloride, Nat. Struct. Mol. Biol. 16 (2009) 334–342.
[3] Y. Umena, K. Kawakami, J.-R. Shen, N. Kamiya, Crystal structure of oxygen-evolving photosystem II at a resolution of 1.9 Å, Nature 473 (2011) 55–60.
[4] B.A. Diner, F. Rappaport, Structure, dynamics, and energetic of the primary photochemistry of photosystem II of oxygenic photosynthesis, Annu. Rev. Plant Biol. 53 (2002) 551–580.
[5] H. Dau, H. Zaharieva, M. Haumann, Recent developments in research on water oxidation by photosystem II, Curr. Op. Chem. Biol. 16 (2012) 3–10.
[6] M.L. Groot, N.P. Pawlowicz, L.J. van Wilderen, J. Breton, I.H. van Stokkum, R. van Grondelle, Initial electron donor and acceptor in isolated photosystem II reaction centers identified with femtosecond mid-IR spectroscopy, Proc. Natl. Acad. Sci. U. S. A. 102 (2005) 13087–13092.
[7] A.R. Holzwarth, M.G. Muller, M. Reus, M. Nowaczyk, J. Sander, M. Rogner, Kinetics and mechanism of electron transfer in intact photosystem II and in the isolated reaction center: pheophytin is the primary electron acceptor, Proc. Natl. Acad. Sci. U. S. A. 103 (2006) 6895–6900.
[8] A.R. Crofts, C.A. Wraight, The electrochemical domain of photosynthesis, Biochim. Biophys. Acta 726 (1983) 149–185.
[9] B.R. Velthuys, J. Amesz, Charge accumulation at the reducing side of system 2 of photosynthesis, Biochim. Biophys. Acta 333 (1974) 85–94.
[10] B. Kok, B. Forbush, M. McGloin, Cooperation of charges in photosynthetic O_2 evolution—I. A linear four step mechanism, Photochem. Photobiol. 11 (1970) 457–475.
[11] P. Joliot, B. Kok, Oxygen evolution in photosynthesis, in: Govindjee (Ed.), Bioenergetics of Photosynthesis, Academic Press, New York, 1975, pp. 387–412.
[12] N. Cox, J. Messinger, Reflections on substrate water and dioxygen formation, Biochim. Biophys. Acta 1827 (2013) 1020–1030.
[13] N. Cox, D.A. Pantazis, F. Neese, W. Lubitz, Biological water oxidation, Acc. Chem. Res. (2013), http://dx.doi.org/10.1021/ar3003249, (in press).
[14] A.K. Clarke, A. Soitamo, P. Gustafsson, G. Oquist, Rapid interchange between two distinct forms of cyanobacterial photosystem II reaction-center protein D1 in response to photoinhibition, Proc. Natl. Acad. Sci. U. S. A. 90 (1993) 9973–9977.
[15] S.S. Golden, Light-responsive gene expression in cyanobacteria, J. Bacteriol. 177 (1995) 1651–1654.
[16] J. Komenda, H. Hassan, B.A. Diner, R.J. Debus, J. Barber, P.J. Nixon, Degradation of the photosystem II D1 and D2 proteins in different strains of the cyanobacterium *Synechocystis* PCC 6803 varying with respect to the type and level of *psbA* transcript, Plant Mol. Biol. 42 (2000) 635–645.
[17] C.I. Sicora, S.E. Appleton, C.M. Brown, J. Chung, J. Chandler, A.M. Cockshutt, I. Vass, D.A. Campbell, Cyanobacterial *psbA* families in *Anabaena* and *Synechocystis* encode trace, constitutive, and UVB-induced D1 isoforms, Biochim. Biophys. Acta 1757 (2006) 47–56.
[18] P.B. Kós, Z. Deák, O. Cheregi, I. Vass, Differential regulation of *psbA* and *psbD* gene expression, and the role of the different D1 protein copies in the cyanobacterium *Thermosynechococcus elongatus* BP-1, Biochim. Biophys. Acta 1777 (2008) 74–83.
[19] P. Mulo, C. Sicora, E.-M. Aro, Cyanobacterial *psbA* gene family: optimization of oxygenic photosynthesis, Cell. Mol. Life Sci. 66 (2009) 3697–3710.
[20] C.I. Sicora, F.M. Ho, T. Salminen, S. Styring, E.-M. Aro, Transcription of a "silent" cyanobacterial *psbA* gene is induced by microaerobic conditions, Biochim. Biophys. Acta 1787 (2009) 105–112.

[21] M. Sugiura, Y. Kato, R. Takahashi, H. Suzuki, T. Watanabe, T. Noguchi, F. Rappaport, A. Boussac, Energetics in photosystem II from *Thermosynechococcus elongatus* with a D1 protein encoded by either the *psbA*$_1$ or *psbA*$_3$ gene, Biochim. Biophys. Acta 1797 (2010) 1491–1499.
[22] E. Kiss, P.B. Kos, M. Chen, I. Vass, A unique regulation of the expression of the *psbA*, *psbD*, and *psbE* genes, encoding the D1, D2 and cytochrome b_{559} subunits of the photosystem II complex in the chlorophyll d containing cyanobacterium *Acaryochloris marina*, Biochim. Biophys. Acta 1817 (2012) 1083–1094.
[23] Y. Nakamura, T. Kaneko, S. Sato, M. Ikeuchi, H. Katoh, S. Sasamoto, A. Watanabe, M. Iriguchi, K. Kawashima, T. Kimura, Y. Kishida, C. Kiyokawa, M. Kohara, M. Matsumoto, A. Matsuno, N. Nakazaki, S. Shimpo, M. Sugimoto, C. Takeuchi, M. Yamada, S. Tabata, Complete genome structure of the thermophilic cyanobacterium *Thermosynechococcus elongatus* BP-1, DNA Res. 9 (2002) 123–130.
[24] B. Loll, M. Broser, P.B. Kós, J. Kern, J. Biesiadka, I. Vass, W. Saenger, A. Zouni, Modeling of variant copies of subunit D1 in the structure of photosystem II from *Thermosynechococcus elongatus*, Biol. Chem. 389 (2008) 609–617.
[25] J. Sander, M. Nowaczyk, J. Buchta, H. Dau, I. Vass, Z. Deak, M. Dorogi, M. Iwai, M. Rogner, Functional characterization and quantification of the alternative PsbA copies in *Thermosynechococcus elongatus* and their role in photoprotection, J. Biol. Chem. 285 (2010) 29851–29856.
[26] J.L. Hughes, N. Nicholas, A.W. Rutherford, E. Krausz, T.-L. Lai, A. Boussac, M. Sugiura, D1 protein variants in photosystem II from *Thermosynechococcus elongatus* studied by low temperature optical spectroscopy, Biochim. Biophys. Acta 1797 (2010) 11–19.
[27] M. Sugiura, E. Iwai, H. Hayashi, A. Boussac, Differences in the interactions between the subunits of photosystem II dependant on D1 protein variants in the thermophilic cyanobacterium *Thermosynechococcus elongatus*, J. Biol. Chem. 285 (2010) 30008–30018.
[28] A. Boussac, M. Sugiura, F. Rappaport, Probing the quinone binding site of photosystem II from *Thermosynechococcus elongatus* containing either PsbA1 or PsbA3 as the D1 protein through the binding characteristics of herbicides, Biochim. Biophys. Acta 1807 (2010) 119–129.
[29] S. Ogami, A. Boussac, M. Sugiura, Deactivation processes in PsbA1-Photosystem II and PsbA3-Photosystem II under photoinhibitory conditions in the cyanobacterium *Thermosynechococcus elongatus*, Biochim. Biophys. Acta 1817 (2012) 1322–1330.
[30] Y. Kato, T. Shibamoto, S. Yamamoto, T. Watanabe, N. Ishida, M. Sugiura, F. Rappaport, A. Boussac, Influence of the PsbA1/PsbA3 and Ca^{2+}/Sr^{2+} or Cl^-/Br^- exchanges on the redox potential of the primary quinone Q_A in photosystem II as revealed by spectroelectrochemistry, Biochim. Biophys. Acta 1817 (2012) 1998–2004.
[31] M. Sugiura, S. Ogami, M. Kusumi, S. Un, F. Rappaport, A. Boussac, Environment of Tyr_Z in photosystem II from *Thermosynechococcus elongatus* in which PsbA2 is the D1 protein, J. Biol. Chem. 287 (2012) 13336–13347.
[32] M. Sugiura, Y. Inoue, Highly purified thermo-stable oxygen evolving photosystem II core complex from the thermophilic cyanobacterium *Synechococcus elongatus* having His-tagged CP43, Plant Cell Physiol. 40 (1999) 1219–1231.
[33] M. Sugiura, A. Boussac, T. Noguchi, F. Rappaport, Influence of histidine-198 of the D1 subunit on the properties of the primary electron donor, P_{680}, of photosystem II in *Thermosynechococcus elongatus*, Biochim. Biophys. Acta 1777 (2008) 331–342.
[34] M. Sugiura, S. Harada, T. Manabe, H. Hayashi, Y. Kashino, A. Boussac, Psb30 contributes to structurally stabilise the photosystem II complex in the thermophilic cyanobacterium *Thermosynechococcus elongatus*, Biochim. Biophys. Acta 1797 (2010) 1546–1554.
[35] M. Ikeuchi, Y. Inoue, A new 4.8-kDa polypeptide intrinsic to the PS II reaction center, as revealed by modified SDS-PAGE with improved resolution of low-molecular-weight proteins, Plant Cell Physiol. 29 (1988) 1233–1239.
[36] C.A. Kerfeld, M.R. Sawaya, H. Bottin, K.T. Tran, M. Sugiura, D. Cascio, A. Desbois, T.O. Yeates, D. Kirilovsky, A. Boussac, Structural and EPR characterization of the soluble form of cytochrome c-550 and of the *psbV2* gene product from the cyanobacterium *Thermosynechococcus elongatus*, Plant Cell Physiol. 44 (2003) 697–706.
[37] C.A. Kerfeld, S. Yoshida, K.T. Tran, T. Yeates, D. Cascio, H. Bottin, C. Berthomieu, M. Sugiura, A. Boussac, The 1.6 Å resolution structure of Fe-superoxide dismutase from the thermophilic cyanobacterium *Thermosynechococcus elongatus*, J. Biol. Inorg. Chem. 8 (2003) 707–714.
[38] Y. Kashino, W.M. Lauber, J.A. Carroll, Q. Wang, J. Whitmarsh, K. Satoh, H.B. Pakrasi, Proteomic analysis of a highly active photosystem II preparation from the cyanobacterium *Synechocystis* sp. PCC 6803 reveals the presence of novel polypeptides, Biochemistry 41 (2002) 8004–8012.
[39] M.M. Nowaczyk, K. Krause, M. Mieseler, A. Sczibilanski, M. Ikeuchi, M. Rögner, Deletion of *psbJ* leads to accumulation of Psb27–Psb28 photosystem II complexes in *Thermosynechococcus elongatus*, Biochim. Biophys. Acta 1817 (2012) 1339–1345.
[40] L.-X. Shi, M. Hall, C. Funk, W.P. Schröder, Photosystem II, a growing complex: updates on newly discovered components and low molecular mass proteins, Biochim. Biophys. Acta 1817 (2012) 13–25.
[41] R.D. Fagerlund, J.J. Eaton-Rye, The lipoproteins of cyanobacterial photosystem II, J. Photochem. Photobiol. B Biol. 104 (2011) 191–203.
[42] S. Sakata, N. Mizusawa, H. Kubota-Kawai, I. Sakurai, H. Wada, Psb28 is involved in recovery of photosystem II at high temperature in *Synechocystis* sp. PCC 6803, Biochim. Biophys. Acta 1827 (2013) 50–59.
[43] N. Keren, H. Ohkawa, E.A. Welsh, M. Liberton, H.B. Pakrasi, Psb29, a conserved 22-kD protein, functions in the biogenesis of photosystem II complexes in *Synechocystis* and *Arabidopsis*, Plant Cell 17 (2005) 2768–2781.
[44] J. Komenda, J. Nickelsen, M. Tichy, O. Prasil, L.A. Eichacker, P.J. Nixon, The cyanobacterial homologue of HCF136/YCF48 is a component of an early photosystem II assembly complex and is important for both the efficient assembly and repair of photosystem II in *Synechocystis* sp. PCC 6803, J. Biol. Chem. 283 (2008) 22390–22399.
[45] H. Liu, J. Chen, R.Y.-C. Huang, D. Weisz, M.L. Gross, H.B. Pakrasi, Mass spectrometry-based footprinting reveals structural dynamics of loop E of the chlorophyll-binding protein CP43 during photosystem II assembly in the cyanobacterium *Synechocystis* 6803, J. Biol. Chem. 288 (2013) 14212–14220.
[46] F. Michoux, K. Takasaka, M. Boehm, P.J. Nixon, J.W. Murray, Structure of CyanoP at 2.8 angstrom: implications for the evolution and function of the PsbP subunit of photosystem II, J. Biol. Chem. 283 (2008) 22390–22399.
[47] F. Michoux, K. Takasaka, M. Boehm, J. Komenda, P.J. Nixon, J.W. Murray, Crystal structure of the Psb27 assembly factor at 1.6: implications for binding to photosystem II, Photosynth. Res. 110 (2012) 169–175.
[48] Y.H. Yang, T.A. Ramelot, J.R. Cort, D.Y. Wang, C. Ciccosanti, K. Hamilton, R. Nair, B. Rost, T.B. Acton, R. Xiao, J.K. Everett, G.T. Montelione, M.A. Kennedy, Solution NMR structure of photosystem II reaction center protein Psb28 from *Synechocystis* sp. strain PCC 6803, Proteins 79 (2011) 340–344.
[49] A. Boussac, M. Sugiura, Y. Inoue, A.W. Rutherford, EPR study of the oxygen evolving complex in His-tagged photosystem II from the cyanobacterium *Synechococcus elongatus*, Biochemistry 39 (2000) 13788–13799.
[50] J. Peisach, W.E. Blumberg, A. Adler, Electron paramagnetic resonance studies of iron porphyrin and chlorin systems, Ann. N. Y. Acad. Sci. 206 (1973) 310–327.
[51] G. Palmer, The electron paramagnetic resonance of metalloproteins, Biochem. Soc. Trans. 13 (1985) 548–560.
[52] F.A. Walker, Magnetic spectroscopic (EPR, ESEEM, Mossbauer, MCD and NMR) studies of low-spin ferriheme centers and their corresponding heme proteins, Coord. Chem. Rev. 186 (1999) 471–534.
[53] N.A. Tarboush, S. Shin, J. Geng, A. Liu, V.L. Davidson, Effects of the loss of the axial tyrosine ligand of the low-spin heme of MauG on its physical properties and reactivity, FEBS Lett. 586 (2012) 4339–4343.
[54] T. Uchida, J.M. Stevens, O. Daltrop, E.M. Harvat, L. Hong, S.J. Ferguson, T. Kitagawa, The interaction of covalently bound heme with the cytochrome c maturation protein CcmE, J. Biol. Chem. 279 (2004) 51981–51988.
[55] J.M. Stevens, D.A.I. Mavridou, R. Hamer, P. Kritsiligkou, A.D. Goddard, S.J. Ferguson, Cytochrome c biogenesis system I, FEBS J. 278 (2011) 4170–4178.
[56] P.A. Williams, V. Fulop, E.F. Garman, N.F.W. Saunders, S.J. Ferguson, J. Hajdu, Haem-ligand switching during catalysis in crystals of a nitrogen-cycle enzyme, Nature 389 (1997) 406–412.
[57] P. Arnoux, R. Haser, N. Izadi, A. Lecroisey, M. Delepierre, C. Wandersman, M. Czjzek, The crystal structure of HasA, a hemophore secreted by *Serratia marcescens*, Nat. Struct. Biol. 6 (1999) 516–520.
[58] S. Rogers, R. Wells, M. Rechsteiner, Amino acid sequences common to rapidly degraded proteins: the PEST hypothesis, Science 234 (1986) 364–368.
[59] J. Simon, L. Hederstedt, Composition and function of cytochrome c biogenesis system II, FEBS J. 278 (2011) 4179–4188.
[60] C. de Vitry, Cytochrome c maturation system on the negative side of bioenergetic membranes: CCB or System IV, FEBS J. 278 (2011) 4189–4197.
[61] J.W.A. Allen, Cytochrome c biogenesis in mitochondria—Systems III and V, FEBS J. 278 (2011) 4198–4216.